Statistical analysis of nuclear low-lying states and neutrinoless double-beta decay with a covariant energy density functional

Xin Zhang

collaborators: C. C. Wang, C. R. Ding, and J. M. Yao

DFT2025. 2025.3.25

Neutrinoless double-beta decay ($0\nu\beta\beta$)

✓ $0\nu\beta\beta$ decay:

$$(Z, A) \to (Z+2, A) + 2e^-$$

- The half-life of $0\nu\beta\beta$ decay in the standard mechanism of light neutrino exchange is:

$$\left(T^{0\nu}_{1/2}\right)^{-1} = G_{0\nu} \cdot \left|\frac{\langle m_{\beta\beta}\rangle}{m_e}\right|^2 \left|M^{0\nu}\right|^2$$

- The matrix element (NME) is:

$$M^{0\nu} = \left\langle \Psi_f \middle| O^{0\nu} \middle| \Psi_i \right\rangle .$$

J, M, Yao *et al.*, PPNP. 126, 103965 (2022)

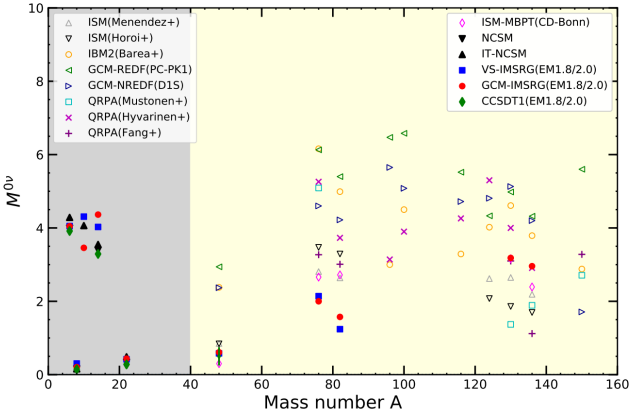

Various nuclear models predict NMEs that differ by three to more!

We need to perform correlation analysis and uncertainty quantification for each model to understand this discrepancy, which requires expensive calculations.

The source of uncertainty

- Systematic error: due to imperfect modeling: deficient parametrizations, wrong assumptions, and missing physics due to our lack of knowledge;
- Statistical error: for a fixed model, statistical error refers to the model quality deviation caused by the parameters that determine the model. By studying the statistical error of parameters, the statistical error under fixed model can be given.

J Dobaczewski *et al.*, J. Phys. G: Nucl. Part. Phys. 41 074001 (2014)

The task of this work is to analyze the statistical uncertainty of observables based on the framework of multi-reference covariant density functional theory (MR-CDFT).

✓ Analysis approaches: Monte Carlo simulation PRC. 110, 064606 (2024), Gaussian process PRL. 132, 182502 (2024), Bayesian posterior analysis Nature Physics, 18, 1196–1200 (2022)...

Covariant Density Functional Theory (CDFT)

- The CDFT starts from the following energy density functional (EDF) under the mean-field approximation:

$$E_{\rm tot} = E_{\rm DF}\left[\boldsymbol{\tau}, \rho_S, j_i^\mu, A_\mu\right] + E_{\rm pair}\left[\kappa, \kappa^*\right] + E_{\rm cm}^{\rm mic}$$
$$= \int d^3r \left(\mathcal{E}^{\rm kin}(\boldsymbol{r}) + \mathcal{E}^{\rm int}(\boldsymbol{r}) + \mathcal{E}^{\rm em}(\boldsymbol{r})\right) - \sum_{\tau=n,p} \frac{V_\tau}{4} \int d^3r \kappa_\tau^*(\boldsymbol{r})\kappa_\tau(\boldsymbol{r}) + E_{\rm cm}^{\rm mic}$$

- The interaction part with low-energy constants $\mathbf{C} = \{\alpha_S, \beta_S, \gamma_S, \delta_S, \alpha_V, \gamma_V, \delta_V, \alpha_{TV}, \delta_{TV}\}$:

$$\begin{aligned}\mathcal{E}^{\rm int}(\boldsymbol{r}) =& \frac{\alpha_S}{2}\rho_S^2 + \frac{\beta_S}{3}\rho_S^3 + \frac{\gamma_S}{4}\rho_S^4 + \frac{\delta_S}{2}\rho_S\Delta\rho_S \\ &+ \frac{\alpha_V}{2}j_\mu j^\mu + \frac{\gamma_V}{4}\left(j_\mu j^\mu\right)^2 + \frac{\delta_V}{2}j_\mu \Delta j^\mu \\ &+ \frac{\alpha_{TV}}{2}\vec{j}_{TV}^{\,\mu}\cdot\left(\vec{j}_{TV}\right)_\mu + \frac{\delta_{TV}}{2}\vec{j}_{TV}^{\,\mu}\cdot\Delta\left(\vec{j}_{TV}\right)_\mu\end{aligned}$$

- The local densities $\rho_S(\boldsymbol{r})$ and currents $j_V^\mu(\boldsymbol{r})$, $\vec{j}_{TV}^{\,\mu}(\boldsymbol{r})$ and pairing tensor $\kappa(\boldsymbol{r})$ are:

$$\rho_S(\boldsymbol{r}) = \sum_k v_k^2 \bar{\psi}_k(\boldsymbol{r})\psi_k(\boldsymbol{r}) \quad , \quad j_V^\mu(\boldsymbol{r}) = \sum_k v_k^2 \bar{\psi}_k(\boldsymbol{r})\gamma^\mu\psi_k(\boldsymbol{r})$$

$$\vec{j}_{TV}^{\,\mu}(\boldsymbol{r}) = \sum_k v_k^2 \bar{\psi}_k(\boldsymbol{r})\vec{\tau}\gamma^\mu\psi_k(\boldsymbol{r}) \quad , \quad \kappa(\boldsymbol{r}) = -2\sum_{k>0} f_k u_k v_k \left|\psi_k(\boldsymbol{r})\right|^2$$

Generator Coordinate Method (GCM)

- The GCM wave function is expanded on a set of non-orthogonal basis for a certian EDF:
  P. Ring and P. Schuck, The nuclear many-body problem (1980)

$$\left|\Psi_{\nu}^{JNZ}\right\rangle = \sum_{\mathbf{q}}^{N_{\mathbf{q}}} f_{\nu}^{JNZ}(\mathbf{q}) \left|JNZ;\mathbf{q}\right\rangle ,$$

  where $|JNZ;\mathbf{q}\rangle \equiv \hat{P}^{J}_{M,K=0}\hat{P}^{N}\hat{P}^{Z}|\Phi(\mathbf{q})\rangle$ are symmetry-projected quasiparticle vacua.

- The variational principle yields the Hill-Wheeler-Griffin (HWG) equation:

$$\sum_{\mathbf{q}'}\left[\mathcal{H}(\mathbf{q},\mathbf{q}') - E_{\nu}^{JNZ}\mathcal{N}(\mathbf{q},\mathbf{q}')\right] f_{\nu}^{JNZ}(\mathbf{q}') = 0,$$

  which contains norm kernels $\mathcal{N}$ and Hamiltonian kernels $\mathcal{H}$.

The CDFT+GCM (MR-CDFT) method entails an extensive computational burden, thereby rendering the statistical uncertainty analysis exceedingly challenging.

Eigenvector continuation(EC)

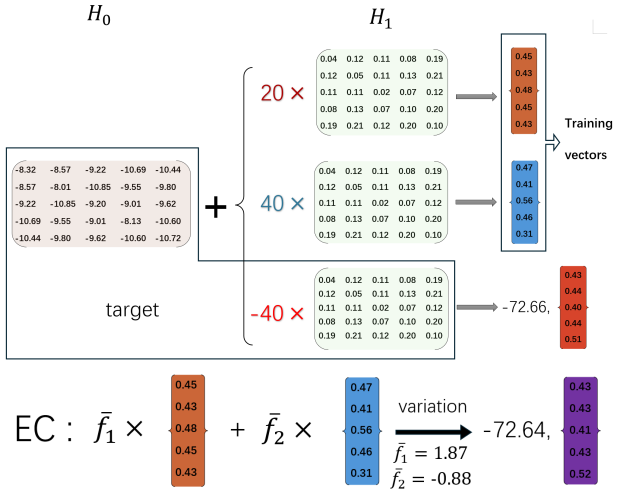

✓ The core idea of EC is that the ground state eigenvector for the given Hamiltonian family $H(c) = H_0 + cH_1$ can be extended to eigenvectors at the training points:

$$|\Psi_{g.s}(c)\rangle = \sum_{c_i} \bar{f}(c_i)|\Psi_{g.s}(c_i)\rangle$$

PRL 121, 032501 (2018)

- In SP-CDFT, the wave function $\left|\bar{\Psi}^{JNZ}(\mathbf{C}_\odot)\right\rangle$ of a target EDF $E_{\mathbf{C}_\odot}(\boldsymbol{\rho}) = E_0(\boldsymbol{\rho}) + \mathbf{C}_\odot \cdot \boldsymbol{\rho}$ is expanded in terms of the basis wave functions $\left|\Psi_\nu^{JNZ}(\mathbf{C}_t)\right\rangle$ of the first $k_{\max}$ states by the N_t training EDFs,

$$\left|\bar{\Psi}_k^{JNZ}(\mathbf{C}_\odot)\right\rangle = \sum_{\nu=1}^{k_{\max}} \sum_{t=1}^{N_t} \bar{f}_{k,\mathbf{C}_\odot}^{JNZ}(\nu, \mathbf{C}_t) \left|\Psi_\nu^{JNZ}(\mathbf{C}_t)\right\rangle,$$

- The mixing coefficient $\bar{f}_{k,\mathbf{C}_\odot}^{JNZ}(\nu, \mathbf{C}_t)$ is determined by the following equation,

$$\sum_{\nu'=1}^{k_{\max}} \sum_{t'=1}^{N_t} \left[\mathscr{H}_{tt'}^{\nu\nu'}(\mathbf{C}_\odot) - \bar{E}_{k,\mathbf{C}_\odot}^{JNZ} \mathscr{N}_{tt'}^{\nu,\nu'} \right] \bar{f}_{k,\mathbf{C}_\odot}^{JNZ}(\nu', \mathbf{C}_{t'}) = 0,$$

- Here, we define the norm and Hamiltonian kernels of the EC method for a target EDF,

$$\mathscr{N}_{tt'}^{\nu\nu'} = \left\langle \Psi_\nu^{JNZ}(\mathbf{C}_t) \right| \left. \Psi_{\nu'}^{JNZ}(\mathbf{C}_{t'}) \right\rangle,$$
$$\mathscr{H}_{tt'}^{\nu\nu'}(\mathbf{C}_\odot) = \left\langle \Psi_\nu^{JNZ}(\mathbf{C}_t) \right| \hat{H}(\mathbf{C}_\odot) \left| \Psi_{\nu'}^{JNZ}(\mathbf{C}_{t'}) \right\rangle.$$

- $\mathscr{H}^{\nu\nu'}_{tt'}(\mathbf{C}_\odot) = \sum_{\mathbf{q},\mathbf{q}'} f^{JNZ}_{\nu}(\mathbf{q},\mathbf{C}_t) f^{JNZ}_{\nu'}(\mathbf{q}',\mathbf{C}_{t'}) \langle JNZ;\mathbf{q},\mathbf{C}_t|\,\hat{H}(\mathbf{C}_\odot)\,|JNZ;\mathbf{q}',\mathbf{C}_{t'}\rangle$,

  $\langle JNZ;\mathbf{q},\mathbf{C}_t|\,\hat{H}(\mathbf{C}_\odot)\,|JNZ;\mathbf{q}',\mathbf{C}_{t'}\rangle = \frac{2J+1}{2}\int d^J_{00}(\cos\theta)d(\cos\theta)\int\frac{e^{-iN\varphi_n}}{2\pi}d\varphi_n\int\frac{e^{-iN\varphi_p}}{2\pi}d\varphi_p$
  $\times\langle\Phi(\mathbf{q},\mathbf{C}_t)|\,\hat{H}(\mathbf{C}_\odot)e^{i\theta\hat{J}_y}e^{i\varphi_n\hat{N}}e^{i\varphi_p\hat{Z}}\,|\Phi(\mathbf{q}',\mathbf{C}_{t'})\rangle$,

- The energy overlap which is evaluated with the mixed-density prescription,

$$\frac{\langle\Phi(\mathbf{q},\mathbf{C}_t)|\,\hat{H}(\mathbf{C}_\odot)e^{i\theta\hat{J}_y}e^{i\varphi_n\hat{N}}e^{i\varphi_p\hat{Z}}\,|\Phi(\mathbf{q}',\mathbf{C}_{t'})\rangle}{\langle\Phi(\mathbf{q},\mathbf{C}_t)|\,e^{i\theta\hat{J}_y}e^{i\varphi_n\hat{N}}e^{i\varphi_p\hat{Z}}\,|\Phi(\mathbf{q}',\mathbf{C}_{t'})\rangle} = \int d^3r\Big[\tilde{\tau}(\boldsymbol{r})+\tilde{\mathcal{E}}^{\mathrm{em}}(\boldsymbol{r})+\sum_{\ell=1}^{9}c^{\odot}_{\ell}\tilde{\mathcal{E}}^{NN}_{\ell}(\boldsymbol{r})\Big].$$

- Only the interaction energy term depends on the parameters $c^{\odot}_{\ell}$ of the target EDF,

$$\sum_{\ell=1}^{9}c^{\odot}_{\ell}\tilde{\mathcal{E}}^{NN}_{\ell}(\mathbf{q},\mathbf{C}_t;\mathbf{q}',\mathbf{C}_{t'}) = \frac{\alpha^{\odot}_S}{2}\tilde{\rho}^2_S+\frac{\alpha^{\odot}_V}{2}\tilde{j}_\mu\tilde{j}^\mu+\frac{\alpha^{\odot}_{TV}}{2}\vec{\tilde{J}}^\mu_{TV}\cdot(\vec{\tilde{J}}_{TV})_\mu+\cdots$$

  where $\tilde{\rho}_S, \tilde{j}^\mu, \tilde{J}^\mu_{TV}$ are the mixed densities and currents.

SP-CDFT (computational time)

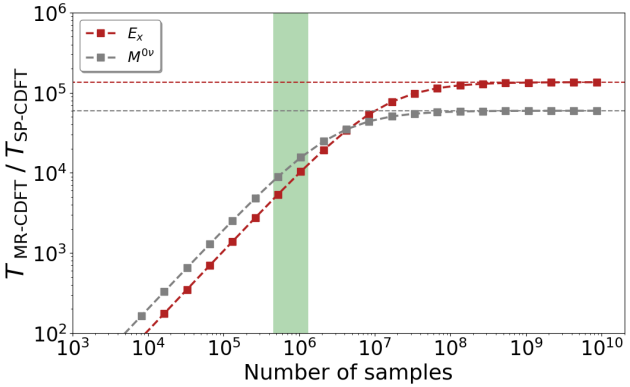

FIG. The ratio of the computation time of MR-CDFT calculation to that of SP-CDFT calculation for ^{150}Nd.

- The number of samples we sample is about 10^6, and the calculated ratio of $T_{\mathrm{MR-CDFT}}/T_{\mathrm{SP-CDFT}} \simeq 10^4$ for ^{150}Nd.
- The SP-CDFT allows us within half an hour using a PC, to predict nuclear low-lying states for 1.3 millions of EDF samples which would otherwise take years with the MR-CDFT.

Benchmark calculation using 64 testing set (^{150}Nd)

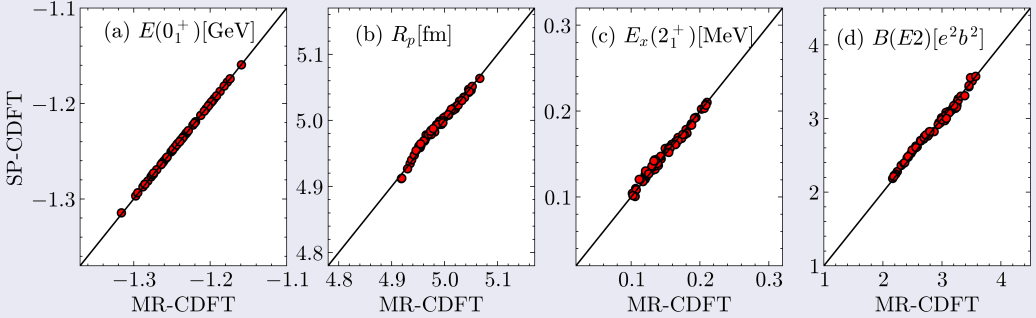

- The relative error for the ground state properties are all within 0.3%.
- The relative error for the low-lying states properties are all within 13%: due to the overlap of errors between the ground state and the lower-lying state.

SP-CDFT (hyperparameters)

✓ we use the symbol SP-CDFT($N_t, k_{\max}$) to mark the number of two hyperparameters.

✓ we introduce a scaling factor $f(c_\ell) = c_\ell / c_\ell^0$ for each parameter in **C**, where c_ℓ^0 is the value of the coupling constant c_ℓ in the PC-PK1.

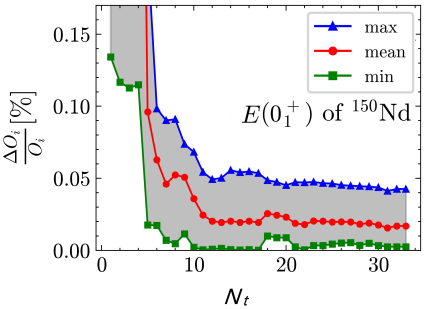

FIG. The relative errors of the ground-state energy of ^{150}Nd from the SP-CDFT(N_t, 3) calculations for the 64 testing sets as the function of N_t.

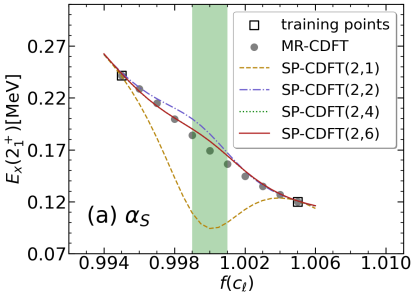

FIG. The comparison of $E_x(2_1^+)$ in ^{150}Nd from MR-CDFT and SP-CDFT($2, k_{\max}$) calculations with different values of $k_{\max}$, as a function of $f(c_\ell)$ for α_S.

SP-CDFT (sampling range)

parameters	value	uncorr. error [%]	Train. range [%]
α_S	-3.96291·10^{-4}	0.83	0.5
β_S	8.6653·10^{-11}	4.7	2
γ_S	-3.80724·10^{-17}	14	4
δ_S	-1.09108·10^{-10}	23	20
α_V	2.69040·10^{-4}	1.2	0.8
γ_V	-3.64219·10^{-18}	54	30
δ_V	-4.32619·10^{-10}	76	20
α_{TV}	2.95018·10^{-5}	11	10
δ_{TV}	-4.11112·10^{-10}	1700	150

Phys. Rev. C 82, 054319 (2010)

✓ The ranges for sampling of the parameters are chosen according to the uncorrelated tolerance of parameters with $\chi^2 \leq \chi^2_{\min} + 1$;
Phys. Rev. C 65, 044308 (2002)

✓ 14 training N_t using Latin hypercube sampling;

✓ 1.3 million samples using quasi Monte-Carlo (MC) sampling with a uniform distribution.

SP-CDFT (global sensitivity analysis)

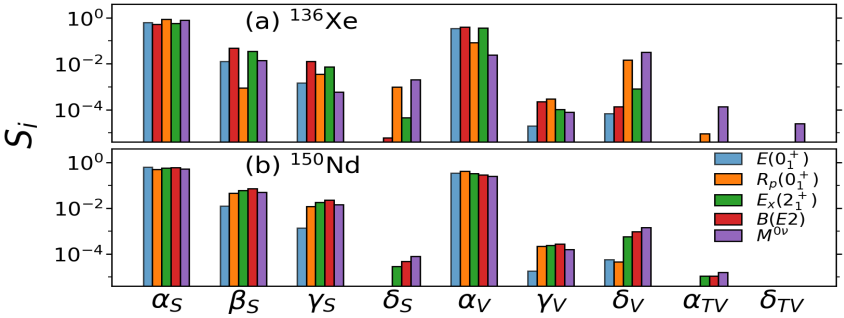

- We sample a parameter domain corresponding to a 0.5% variation around the PC-PK1 value.
- The sensitivity of a parameter is calculated by:

$$S_i = \frac{V_i}{\sum_{i=1}^{d} V_i + \sum_{i<j}^{d} V_{ij} + \cdots + V_{12\ldots d}}$$

where $V_i = \mathrm{Var}\left(E_{\mathbf{C}_{\tilde{i}}}(Y \mid c_i)\right)$ denotes the variance of $E_{\mathbf{C}_{\tilde{i}}}(Y \mid c_i)$, which is the conditional expectation of Y for the i-th parameter, $E_{\mathbf{C}_{\tilde{i}}}(Y \mid c_i) = \frac{1}{N_Y}\sum_{n=1}^{N_Y} Y^{(n)}(\mathbf{C}_{\tilde{i}})$.

SP-CDFT (correlation analysis)

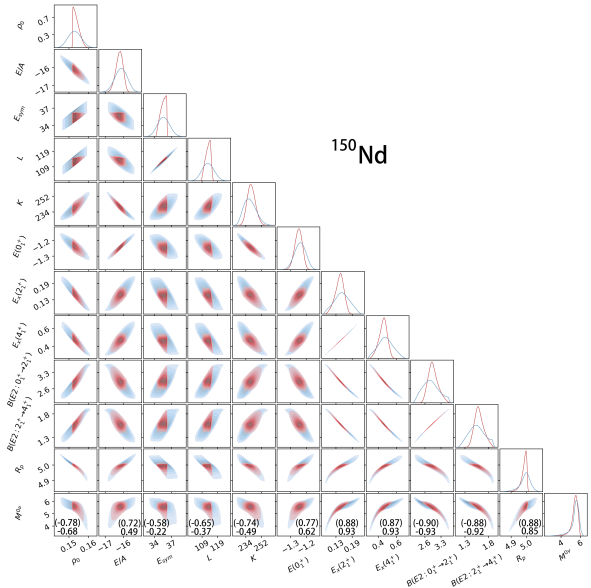

✓ Samples of EDFs: 1,310,720 (in blue).
✓ Samples of EDFs refined with the nuclear matter properties: 457,380 (in red).

Correlation Analysis

- There are strong correlations between R_p and ρ_0, $E(0_1^+)$ and E/A.
- The excitation energies of the 2_1^+ and 4_1^+ states are anti-correlated with the $E2$ transition strengths; the proton radius R_p of the ground state is positively anti-correlated with the $B(E2: 0_1^+ \to 2_1^+)$
- The correlations of the quantities for nuclear matter with $M^{0\nu}$ are weak.
- There are rather strong correlations between the $M^{0\nu}$ and nuclear low-lying states.

SP-CDFT (correlation analysis)

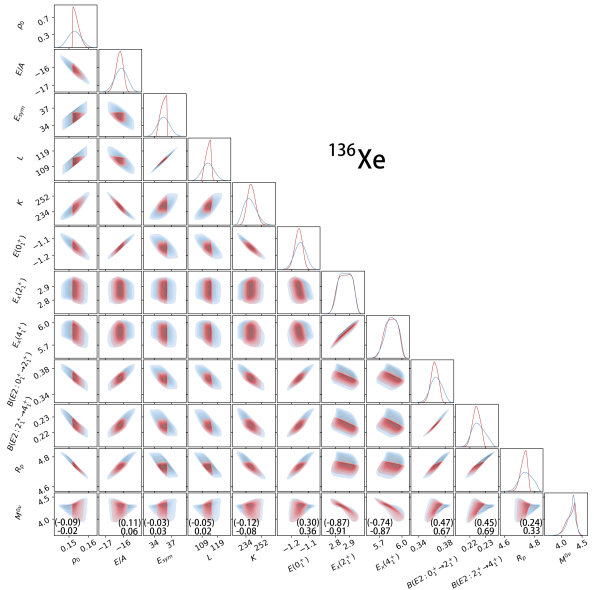

✓ Samples of EDFs: 1,310,720 (in blue).
✓ Samples of EDFs refined with the nuclear matter properties: 457,380 (in red).

Correlation Analysis

- The excitation energies of the 2_1^+ and 4_1^+ states are weakly correlated with the $E2$ transition strengths due to the spherical nuclei; the proton radius R_p of the ground state is positively correlated with the $B(E2:0_1^+\to2_1^+)$
- There are rather strong correlations between the $M^{0\nu}$ and the excitation energy of $2_1^+, 4_1^+$ states, but weak correlations between the $M^{0\nu}$ and $B(E2)$.

SP-CDFT (uncertainty analysis)

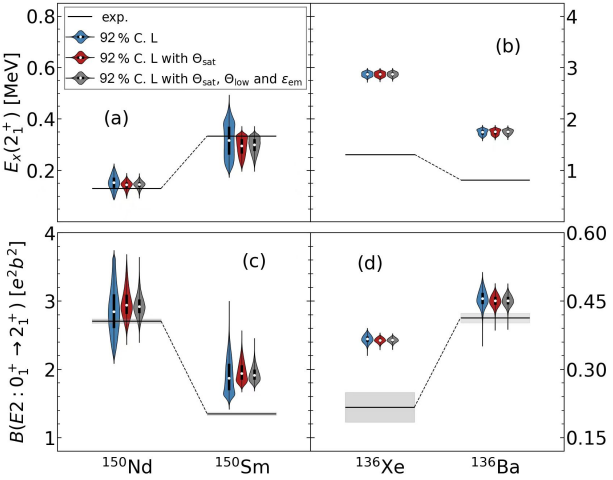

Uncertainty analysis of low-lying states

- The excitation energies and $E2$ transition strengths of ^{150}Nd and ^{150}Sm are reasonably reproduced;
- The collectivity of the single-magic nucleus ^{136}Xe is overestimated due to the lack of particle-hole excitation configurations in the model space.
  C. R. Ding *et al.*, PRC 108, 054304 (2023)
- The statistical uncertainties from the nine parameters in the particle-hole part of the EDF are within 9% for the excitation energies and 5% for the $E2$ transition strengths.

SP-CDFT (uncertainty analysis)

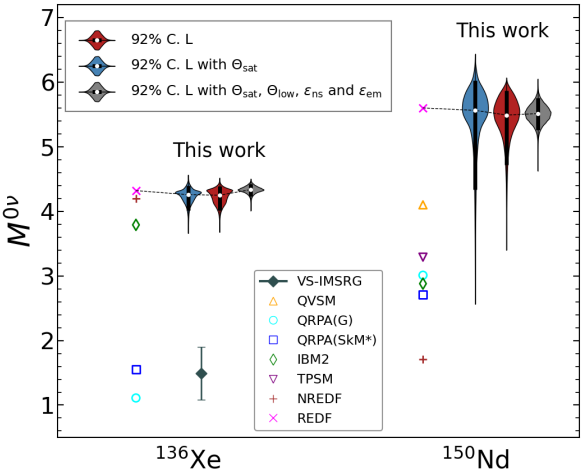

Uncertainty analysis of $M^{0\nu}$

- The use of the information of nuclear matter and nuclear low-lying states in the Bayesian method does not change evidently the NME;
- The final mean value and statistical uncertainty (68% confidence level) of the NME are 5.51(14), and 4.33(5) for ^{150}Nd and ^{136}Xe, respectively, in line with the values 5.60 and 4.32 by the PC-PK1.

J. M. Yao *et al.*, PRC 91, 024316 (2015)

SP-CDFT (uncertainty analysis)

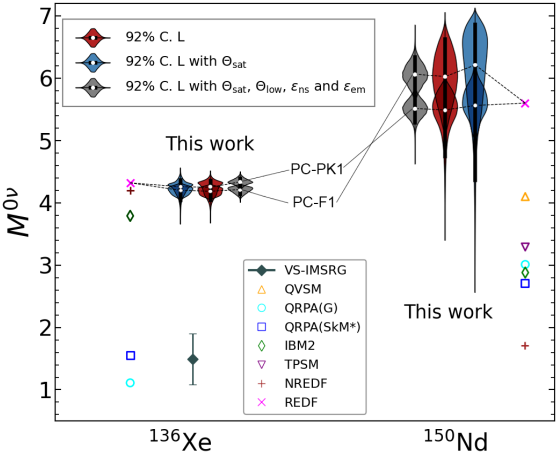

- The final mean value and statistical uncertainty are $4.21^{+0.07}_{-0.10}$ for ^{136}Xe and $6.07^{+0.30}_{-0.32}$ for ^{150}Nd for PC-F1. By using the Bayesian model averaging (BMA) method, we obtain the NMEs of $4.34^{+0.09}_{-0.11}$ for ^{136}Xe and $5.52^{+0.23}_{-0.26}$ for ^{150}Nd.

SP-CDFT (application in high-energy nuclear collisions)

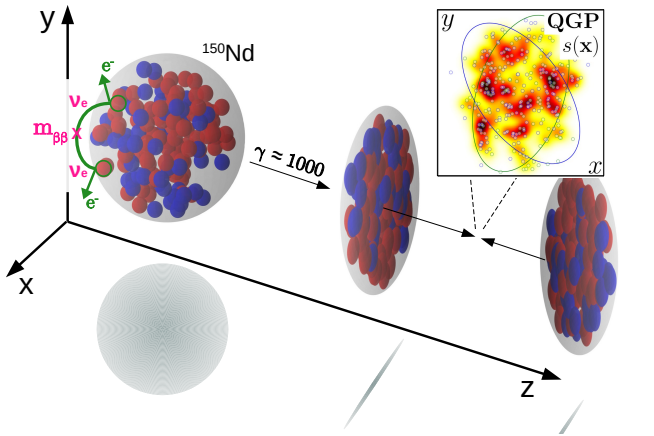

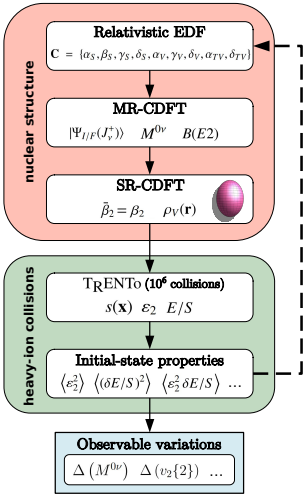

FIG. Collider experiments with isobars provide robust probes of the nuclear geometry.

Y.Li, X. Zhang, G. Giacalone, J. M. Yao, arXiv.2502.08027 [nucl-th] (2025).

SP-CDFT (application in high-energy nuclear collisions)

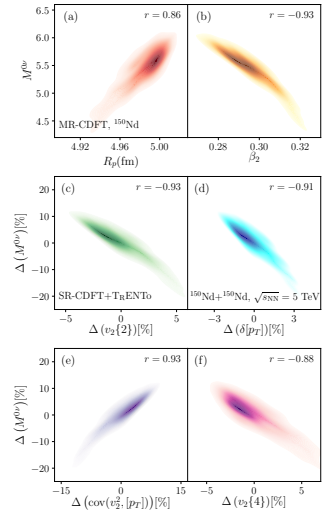

- $\Delta(\mathcal{O}) = (\mathcal{O} - \langle\mathcal{O}\rangle_{\mathbf{C}})/|\langle\mathcal{O}\rangle_{\mathbf{C}}|$,
- ν_2 is the final-state elliptic flow coefficient which reflects the quadrupole deformation of the colliding nuclei,
- p_T is the average hadron momentum which differentiates the spectra of soft hadrons emitted to the final states, revealing nuclear structure effects in ultra-central collisions.

✓ All of these variations are strongly correlated with the value of the NME.

✓ By extending the high-energy data to the Bayesian analysis should effectively improve the extraction of the nuclear deformation.

Summary and Prospect

Summary

- We tested the effectiveness of SP-CDFT method. Then, the SP-CDFT method is applied to calculate different observables under 1.3 million sets of interactions. We use these samples to perform global sensiticity analysis, correlation analysis, and finally give the uncertainty of the low-lying states and $M^{0\nu}$ of ^{150}Nd and ^{136}Xe.
- We reveal prominent correlations between the NME and features of the quark-gluon plasma (QGP) formed in these processes. Our findings demonstrate collider experiments involving $0\nu\beta\beta$ decay candidates as a platform for benchmarking theoretical predictions of the NME.

Prospect

- We expect to analyze the uncertainty of matrix elements of more heavy nuclei and overweight nuclei in low excited state and neutrino-free double beta decay candidates. In addition, we will promote the large-scale application of SP-CDFT in combination with different interactions.
- The results from calculations of heavy-ion collisions have to be followed up by a combined Bayesian analysis of low- and high-energy data.

Thanks!

SP-CDFT (Bayesian analysis)

- The posterior distribution of certain observable $\hat{y}$ is:

$$p(\hat{y}|D) = \int p(\hat{y}|\theta)p(\theta|D)d\theta = \int p(\hat{y}|\theta)\frac{p(D|\theta)\pi(\theta)}{p(D)}d\theta$$

- The prior distribution is constructed as a Gaussian function. The center of Gaussian function is PC-PK1 value (θ^0), and the bandwidth is the variance of sample parameters σ_θ:

$$\pi(\theta) = exp[-(\theta - \theta^0)^2/2\sigma_\theta]$$

- Likelihood function $p(D|\theta)$ is constructed as:

$$p(D|\theta) = exp[-(D - y(\theta))^2/2\sigma]$$

- The σ in the likelihood function includes experimental uncertainty σ_{exp}, emulator error of SP-CDFT σ_{em}:

$$\sigma = \sigma_{exp} + \sigma_{em}$$

  Where σ_{em} is given by the minimum variance unbiased estimator (MVUE)。

Giuliani, Pablo and Godbey, Kyle and Bonilla, Edgard and Viens, Frederi and Piekarewicz, Jorge, Front. Phys, 2022.1054524(2023)

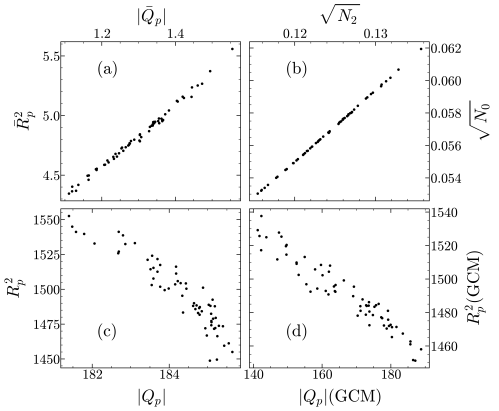

FIG. (a), (b), (c) The correlations among mean-squared radius $R_p^2 = N_0^{-1} \langle J = 0NZ; \beta_2, \mathbf{C}| \hat{R}_p^2 |J = 0NZ; \beta_2, \mathbf{C}\rangle$, reduced $E2$ transition matrix element $Q_p = (N_0 N_2)^{-1/2} \langle J = 2NZ; \beta_2, \mathbf{C}| |\hat{Q}_2| |J = 0NZ; \beta_2, \mathbf{C}\rangle$ and normalization factors $\sqrt{N_J}$ from the calculations for ^{150}Nd based on a single configuration with $\beta_2 = 0.3$, where $N_J = \langle JNZ; \beta_2, \mathbf{C}| JNZ; \beta_2, \mathbf{C}\rangle$. (d) The results from the configuration-mixing GCM calculations. The quantities hatted with bars are unnormalized.

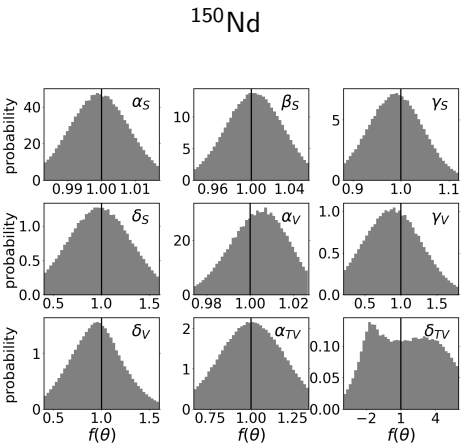
^{150}Nd
probability
α_S
β_S
γ_S
δ_S
α_V
γ_V
δ_V
α_{TV}
δ_{TV}
$f(\theta)$

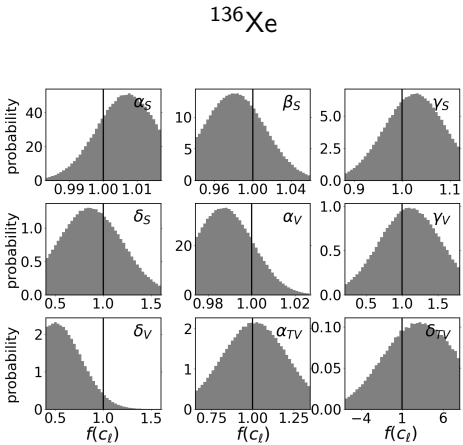
^{136}Xe
probability
α_S
β_S
γ_S
δ_S
α_V
γ_V
δ_V
α_{TV}
δ_{TV}
$f(c_t)$